

REPORT DOCUMENTATION PAGE				Form Approved OMB NO. 0704-0188	
<p>The public reporting burden for this collection of information is estimated to average 1 hour per response, including the time for reviewing instructions, searching existing data sources, gathering and maintaining the data needed, and completing and reviewing the collection of information. Send comments regarding this burden estimate or any other aspect of this collection of information, including suggestions for reducing this burden, to Washington Headquarters Services, Directorate for Information Operations and Reports, 1215 Jefferson Davis Highway, Suite 1204, Arlington VA, 22202-4302. Respondents should be aware that notwithstanding any other provision of law, no person shall be subject to any penalty for failing to comply with a collection of information if it does not display a currently valid OMB control number.</p> <p>PLEASE DO NOT RETURN YOUR FORM TO THE ABOVE ADDRESS.</p>					
1. REPORT DATE (DD-MM-YYYY) 31-08-2009		2. REPORT TYPE Final Report		3. DATES COVERED (From - To) 1-Sep-2005 - 31-Aug-2009	
4. TITLE AND SUBTITLE Ab initio study of ultracold polar molecules in optical lattices				5a. CONTRACT NUMBER W911NF-05-1-0472	
				5b. GRANT NUMBER	
				5c. PROGRAM ELEMENT NUMBER 611102	
6. AUTHORS Svetlana Kotochigova				5d. PROJECT NUMBER	
				5e. TASK NUMBER	
				5f. WORK UNIT NUMBER	
7. PERFORMING ORGANIZATION NAMES AND ADDRESSES Temple University Sponsored Projects Administration 1601 N Broad Street Philadelphia, PA 19122 -6003				8. PERFORMING ORGANIZATION REPORT NUMBER	
9. SPONSORING/MONITORING AGENCY NAME(S) AND ADDRESS(ES) U.S. Army Research Office P.O. Box 12211 Research Triangle Park, NC 27709-2211				10. SPONSOR/MONITOR'S ACRONYM(S) ARO	
				11. SPONSOR/MONITOR'S REPORT NUMBER(S) 48766-PH.1	
12. DISTRIBUTION AVAILABILITY STATEMENT Approved for public release; federal purpose rights					
13. SUPPLEMENTARY NOTES The views, opinions and/or findings contained in this report are those of the author(s) and should not be construed as an official Department of the Army position, policy or decision, unless so designated by other documentation.					
14. ABSTRACT We described our theoretical advances that influenced the experimental creation of vibrationally and translationally cold polar molecules. Our analysis includes multi-channel bound states of ground and excited electronic states. We have excellent agreement with the hyperfine structure observed in experimental data. In addition, we studied spin-orbit mixing in the intermediate state of the Raman transitions used in experiment. We also obtained the polarizability of the polar molecules near					
15. SUBJECT TERMS polar molecules, photoassociation, optical lattices, alkali-metal and alkaline-earth molecules					
16. SECURITY CLASSIFICATION OF:			17. LIMITATION OF ABSTRACT UU	15. NUMBER OF PAGES	19a. NAME OF RESPONSIBLE PERSON Svetlana Kotochigova
a. REPORT UU	b. ABSTRACT UU	c. THIS PAGE UU			19b. TELEPHONE NUMBER 301-975-8562

## Report Title

Ab initio study of ultracold polar molecules in optical lattices

### ABSTRACT

We described our theoretical advances that influenced the experimental creation of vibrationally and translationally cold polar molecules. Our analysis includes multi-channel bound states of ground and excited electronic states. We excellent agreement with the hyperfine structure observed in experimental data. In addition, we studied spin-orbit mixing in the intermediate state of the Raman transitions used in experiment. We also obtained the polarizability of the polar molecules near frequencies relevant for optical trapping with optical lattices. We then studied the electronic properties of a new class of polar molecules created from collisions of Li and alkaline-earth or rare-earth atoms, such LiSr and LiYb. Finally, we calculated the isotropic and anisotropic interaction potentials between two polar molecules.

---

**List of papers submitted or published that acknowledge ARO support during this reporting period. List the papers, including journal references, in the following categories:**

**(a) Papers published in peer-reviewed journals (N/A for none)**

1. S. Ospelkaus , K.-K. Ni , M. H. G. de Miranda , B. Neyenhuis , D. Wang , S. Kotochigova , P. S. Julienne, D. S. Jin and J. Ye,  
" Ultracold polar molecules near quantum degeneracy",  
Faraday Discuss., 142, 351–359, (2009).
2. S. Kotochigova, E. Tiesinga, and P. S. Julienne,  
" Multi-channel modelling of the formation of vibrationally cold polar KRb molecules",  
New J. Phys. 11, 055043, (2009).
3. S. Kotochigova, T. Zelevinsky, and Jun Ye,  
"Prospects for application of ultracold Sr molecules in precision measurements"  
Phys. Rev. A 79, 012504, (2009).
4. K.-K Ni, S. Ospelkaus, M. H. G. de Miranda, A. Pe'er, B. Neyenhuis, J. J. Zirbel, S. Kotochigova, P. S. Julienne, D. S. Jin, and J. Ye,  
"A high phase-space-density gas of polar molecules in the rovibrational ground state"  
Science 322, 231 (2008).
5. S. Ospelkaus, A. Pe'er, K.-K. Ni, J. J. Zirbel, B. Neyenhuis, S. Kotochigova, P. S. Julienne, J. Ye, and D. S. Jin,  
" Efficient state transfer in an ultracold dense gas of heteronuclear molecules"  
Nature Physics 4, 622 (2008).
6. E. R. Hudson, N. B. Gilfoy, S. Kotochigova, J. M. Sage, and D. DeMille,  
" Inelastic collisions of ultracold heteronuclear molecules in an optical trap"  
Phys. Rev. Lett. 100, 203201 (2008)
7. D. DeMille, S. Sainis, J. Sage, T. Bergeman, S. Kotochigova, and E. Tiesinga,  
"Enhanced sensitivity to variation of  $m_e/m_p$  in molecular spectra"  
Phys. Rev. Lett. 100, 043202 (2008).
8. T. Zelevinsky, S. Kotochigova, and Jun Ye,  
"Precision test of mass-ratio variations with lattice-confined ultracold molecules"  
Phys. Rev. Lett. 100, 043201 (2008).
9. S. Kotochigova,  
"Relativistic electronic structure of the Sr<sub>2</sub> molecule"  
J. Chem. Phys. 128, 024303 (2008).
10. O. Salihoglu, P. Qi, E. H. Ahmed, S. Kotochigova, S. Magnier, and A. M. Lyyra,  
"Comparison of Autler–Townes splitting based absolute measurements  
of the  $7\text{Li}2\text{A }1\Sigma^+ - X\text{ }1\Sigma^+$  electronic transition dipole moment with ab initio theory",  
J. Chem. Phys. 129, 174301 (2008).
11. S. Kotochigova,  
"Prospects for making polar molecules with microwave fields",  
Phys. Rev. Lett. 99, 073003 (2007).
12. P. Qi, J. Bai, E. Ahmed, A. M. Lyyra, S. Kotochigova, A. J. Ross, C. Effantin,  
P. Zalicki, J. Vigue, G. Chawla, W. Field, T.-J. Whang, W. C. Stwalley, H. Knöckel,  
E. Tiemann, J. Shang, L. Li, and T. Bergeman,  
"New spectroscopic data, spin-orbit  
functions, and global analysis of data on the  $\text{A }1\Sigma^+$  and  $\text{b }3\Pi^+$  states of Na<sub>2</sub>"  
J. Chem. Phys. 124, 084308 (2007).
13. S. Kotochigova and E. Tiesinga,  
"Controlling polar molecules in optical lattices"  
Phys. Rev. A 74, 041405(R) (2006).

14. E. Ahmed, A. Hansson, P. Qi, L. Li, T. Kirova, J. Qi, A. Lazoudis, S. Magnier, S. Kotochigova, and M. Lyyra,  
" Measurement of the electronic transition dipole moment by Autler-Townes splitting: comparison of three and four level system excitation  
schemes for the Na\_2 A 1Sigma\_u - X 1Sigma\_g system"  
J. Chem. Phys. 124, 084308 (2006).

15. S. Kotochigova and E. Tiesinga,  
"Ab initio relativistic calculation of the RbCs molecule"  
J. Chem. Phys. 123, 174304 (2005).

Number of Papers published in peer-reviewed journals: 15.00

---

**(b) Papers published in non-peer-reviewed journals or in conference proceedings (N/A for none)**

Number of Papers published in non peer-reviewed journals: 0.00

---

**(c) Presentations**

16 invited talks during the reported period:

1. "Isotropic and anisotropic short range interactions of ultracold polar molecules", COCOMO JILA workshop, July 13 (2009).
2. "What we need to know about ultracold polar molecules", Harvard/MIT CUA Colloquim, March 17 (2009),
3. "Vibrationally-dependent interactions of cold polar molecules", ICTP, Italy, Workshop on Quantum Phenomena and Information: From Atomic to Mesoscopic Systems, May 5 (2008).
4. "Vibrational dependence of collisional and field-induced interactions of cold molecules", NIST, Gaithersburg, Maryland, USA, Colloquim, March 25 (2008).
5. "Effects of collisions and optical lattice fields on ultracold molecules", Stony Brook University, Stony Brook, New York, USA Colloquim, March 10 (2008).
6. "New theoretical findings on cold molecules in optical lattices", DAMOP International Conference, Calgary, Canada, June (2007).
7. "Tunable interactions between polar molecules in optical lattices", International Conference on Few-Body Systems, Cuernavaca, Mexico, March (2007).
8. "Ultracold molecules in optical lattices", DARPA Workshop: Optical Lattice Simulator, Arlington, USA, November, (2006).
9. "Engineering ultracold polar molecules by using optical lattices and microwave fields", US-Japan Joint Seminar on Coherent Quantum Systems, Breckenridge, USA, August (2006).
10. "Relativistic study of X-ray spectra of few-electron ions", International Workshop on Precision Physics of Simple Atomic Systems, Venice, Italy, June (2006).
11. "Ab initio study of Sr<sub>2</sub> molecule", JILA Seminar, Boulder, Colorado, USA, October (2006).
12. "Controlling polar molecules in optical lattices", DARPA workshop: Quantum Computing with Polar Molecules, Arlington, USA, (2005).
13. "Ab initio study of polar molecules in optical lattices", International Workshop on Theory of Ultracold Molecules, Telluride, USA, July (2005).
14. "Creating polar molecules in optical lattices", Yale University, New Haven, Connecticut, USA (2005).
15. "Ab initio study of the spin-orbit coupling in alkali metal dimers", International Workshop on Molecular Spectroscopy, Stony Brook, USA, (2005).
16. "Relativistic study of atoms, ions and molecules", Naval Research Laboratory - Plasma Branch. Washington DC, USA, (2005)

Number of Presentations: 16.00

---

**Non Peer-Reviewed Conference Proceeding publications (other than abstracts):**

Number of Non Peer-Reviewed Conference Proceeding publications (other than abstracts): 0

---

**Peer-Reviewed Conference Proceeding publications (other than abstracts):**

Number of Peer-Reviewed Conference Proceeding publications (other than abstracts): 0

---

**(d) Manuscripts**

Number of Manuscripts: 0.00

Patents Submitted

Patents Awarded

Graduate Students

<u>NAME</u>	<u>PERCENT SUPPORTED</u>
FTE Equivalent:	
Total Number:	

Names of Post Doctorates

<u>NAME</u>	<u>PERCENT SUPPORTED</u>
Maria Linnik	0.25
FTE Equivalent:	0.25
Total Number:	1

Names of Faculty Supported

<u>NAME</u>	<u>PERCENT SUPPORTED</u>	National Academy Member
Svetlana Kotochigova	0.50	No
FTE Equivalent:	0.50	
Total Number:	1	

Names of Under Graduate students supported

<u>NAME</u>	<u>PERCENT SUPPORTED</u>
FTE Equivalent:	
Total Number:	

### Student Metrics

This section only applies to graduating undergraduates supported by this agreement in this reporting period

The number of undergraduates funded by this agreement who graduated during this period: ..... 0.00

The number of undergraduates funded by this agreement who graduated during this period with a degree in science, mathematics, engineering, or technology fields:..... 0.00

The number of undergraduates funded by your agreement who graduated during this period and will continue to pursue a graduate or Ph.D. degree in science, mathematics, engineering, or technology fields:..... 0.00

Number of graduating undergraduates who achieved a 3.5 GPA to 4.0 (4.0 max scale): ..... 0.00

Number of graduating undergraduates funded by a DoD funded Center of Excellence grant for Education, Research and Engineering:..... 0.00

The number of undergraduates funded by your agreement who graduated during this period and intend to work for the Department of Defense ..... 0.00

The number of undergraduates funded by your agreement who graduated during this period and will receive scholarships or fellowships for further studies in science, mathematics, engineering or technology fields: ..... 0.00

### Names of Personnel receiving masters degrees

NAME

Total Number:

### Names of personnel receiving PhDs

NAME

Total Number:

### Names of other research staff

NAME

PERCENT SUPPORTED

FTE Equivalent:

Total Number:

### Sub Contractors (DD882)

### Inventions (DD882)





# Ab initio study of ultracold polar molecules in optical lattices.

S. Kotochigova

Department of Physics, Temple University, Philadelphia, PA 19122

## Contents

<b>1</b>	<b>Statement of Problems studied</b>	<b>1</b>
<b>2</b>	<b>Summary of Most important results</b>	<b>2</b>
2.1	Formation of ultracold KRb molecules . . . . .	2
2.2	Molecular Polarizability . . . . .	6
2.3	Development of a new type of cold molecules . . . . .	8
2.4	Interaction between molecules . . . . .	10

## 1 Statement of Problems studied

The recent successful creation of a high phase-space-density gas of polar  $^{40}\text{K} \ ^{87}\text{Rb}$  molecules [1, 2] has been based on both new experimental and theoretical advances in manipulating and understanding properties of such molecules. This opens up the possibility of studying collective phenomena that rely on the long-range interactions between polar molecules. Future experiments can be envisioned in both weakly confining optical traps as well as optical lattices.

The first goal of this study was to give theoretical support on the experimental creation of vibrationally and translationally cold polar  $^{40}\text{K}^{87}\text{Rb}$  molecules. In particular, we analyzed various factors that can affect this creation including the multi-channel description of the initial, intermediate, and final states of the formation by Raman transitions. Examples of Raman transitions are shown in Fig. 1.

Furthermore, we theoretically investigate the interaction of polar molecules with optical lattices and microwave fields. We demonstrate the existence of frequency windows in the optical domain where the complex internal structure of the molecule does not influence the trapping potential of the lattice. In such frequency windows the Franck-Condon factors are so small that near-resonant interaction of vibrational levels of the molecule with the lattice fields have a negligible contribution to the polarizability, and light-induced decoherences are kept to a minimum. In addition, we show that microwave fields can induce a tunable dipole-dipole interaction between ground-state rotationally symmetric ( $J=0$ ) molecules. Our results are based on *ab initio* relativistic electronic structure calculations of the polar KRb and RbCs molecules combined with calculations of their rovibrational motion.

We also studied the electronic properties and dynamics of a new class of ultracold polar molecules created from collisions of ultracold alkali-metal Li and either an alkaline-earth or rare-earth atoms. Our goal was to theoretically determine the previously unknown electronic properties of the LiMg, LiSr and LiYb molecules. To the best of our knowledge, only LiMg was experimentally investigated [3], which allowed us to compare our predictions for the ground state potential of LiMg with experiment.

Finally, we considered scattering and interaction properties of ultracold polar molecules governed by isotropic van-der-Waals forces and short range scattering parameters. We showed that at low temperature (and in absence of an external electric field) the scattering mechanism between molecules and molecules with atoms has a resonant character for certain short-range parameter values, which can lead to enhanced reaction rates. We present results for two polar molecules with different dipolar properties, KRb and RbCs. The van-der-Waals coefficients for these molecules were obtained by integrating products of dynamic polarizability of the molecules in the ground electronic state over imaginary frequency. We have done so for each vibrational state of the ground electronic state. We show that both isotropic and anisotropic coefficients have a significant contribution from dipole coupling to the excited spectrum. This leads to a dramatic difference in the interaction potentials compared to that previously estimated from the permanent dipole moment. Additionally, we investigated the anisotropic polarizability of rotationless  $J = 0$  polar molecules induced by DC electric fields. This anisotropy appears due to the mixing of the  $J = 0$  level with higher  $J$  levels. As result the trapping potential changes with polarization of the trapping light.

## 2 Summary of Most important results

### 2.1 Formation of ultracold KRb molecules

We search for an efficient production mechanism of KRb molecules using a multi-channel description of both ground and excited states. We assume that KRb molecules are initially in the weakly-bound near-threshold vibrational states formed by a magnetic Feshbach resonance in collisions between ultracold  $^{40}\text{K}$  and  $^{87}\text{Rb}$  atoms. In our coupled-channel calculation of the ground state ro-vibrational structure we used the most accurate ground state potentials available from Ref. [4]. Below we analyze this structure, and perform a comparison with available high-precision measurements [1, 2].

Vibrationally cold molecules are preferably made by transferring population from a Feshbach molecular state. For this transfer we selected the pathway that has been proposed by Stwalley [5], which forms vibrationally cold KRb molecules starting from the highly excited vibrational states using one optical Raman transition and intermediate vibrational levels of the  $3(1)$  potential. This mechanism was also used to create vibrationally cold RbCs molecules in Ref. [6]. Reference [7] has reported an analysis of perturbations of the vibrational levels of the  $3(1)$  potential due to spin-orbit interactions with the neighboring potentials in RbCs.

In the Raman transition the initial and final bound vibrational levels belong to the ground  $X^1\Sigma^+$  and  $a^3\Sigma^+$  states. In KRb these states dissociate to the same  $[\text{Ar}]4s(^2S)+[\text{Kr}]5s(^2S)$  atomic limit. The two states are coupled via hyperfine interactions: the Fermi-contact and electron and nuclear Zeeman interactions for each of the constituent atoms. For each atom the Fermi-contact interaction couples its electron spin, here  $1/2$ , to its nuclear spin. The Zeeman interaction is non-zero since an external magnetic field is used to create Feshbach KRb molecules.

The final states of the Raman transitions are  $v = 0$  levels of the  $X^1\Sigma^+$  and  $a^3\Sigma^+$  potentials. Figure 2 shows the rotational hyperfine and Zeeman structure of the  $v = 0$  level of the  $a^3\Sigma^+$  potential at  $B=545.9$  G as calculated with the coupled-channel method. The black lines are the  $\ell=0$  bound states and the red lines are the  $\ell=2$  bound state. Notice though that the rotational energy splitting is smaller than that due to the hyperfine and Zeeman interaction. This leads to overlapping spectral features. The hyperfine structure of the two partial waves is nearly identical. The main difference is that each  $\ell = 2$  hyperfine feature has within it three lines, which are not resolved in the figure. The splitting between these lines is less than 0.3 GHz and is due to the

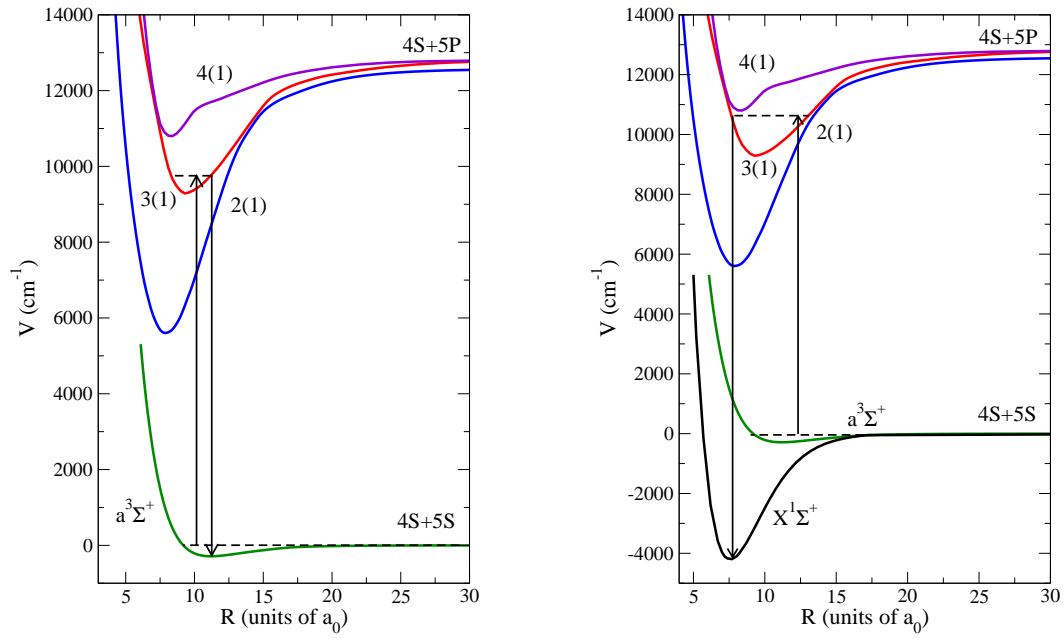


Figure 1: The ground and excited state potential energy curves of  $\text{K Rb}$  that are used for multi-channel modeling as a function of internuclear separation  $R$ . Here  $a_0$  is the Bohr radius of 0.0529 nm.

---

## Final Progress Report

---

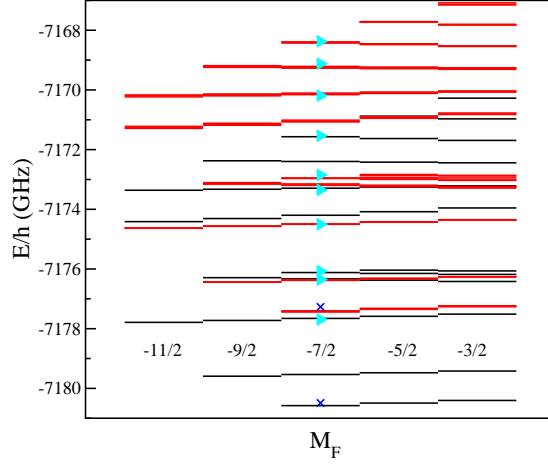


Figure 2: The hyperfine and Zeeman structure at  $B=545.9$  G of the  $\ell=0$  (black lines) and 2 (red lines) rotational levels of the  $v=0$  vibrational state of the  $a^3\Sigma^+$  potential of  $^{40}\text{K}^{87}\text{Rb}$ . The crosses and triangles indicate the experimentally observed energies from Ref. [2]. The theoretical energies have been shifted up by +15.0 GHz to coincide with the experimental data. Zero energy corresponds to the dissociation energy of both  $^{40}\text{K}$  and  $^{87}\text{Rb}$  in the energetically lowest hyperfine state. The levels are grouped by the projection quantum number  $M_F$ . Each  $\ell=2$  hyperfine feature contains three lines, which on the scale of the figure are barely resolved. The splitting is on the order of 0.1 GHz and due to the magnetic spin-spin dipole interaction, which partially lifts the  $m_\ell$  degeneracy of the projection quantum number of  $\vec{\ell}$ .

magnetic spin-spin dipole interaction, which partially lifts the  $m_\ell$  degeneracy of the projection quantum number of  $\vec{\ell}$ . We have performed similar calculations for the  $v=0$  level of the  $X^1\Sigma^+$  state.

The experiments of Refs. [1, 2] have located more than ten sublevels of the  $v=0$  vibrational level of the  $a^3\Sigma^+$  potential. We have compared the calculated hyperfine structure of the  $v=0$  level of the triplet state, shifted up by +15.0 GHz, with the experimental energies of Ref. [2], marked by the crosses and triangles in Fig. 2. The agreement is good.

For the vibrational levels used as intermediate states the 3(1) potential can to first order be described as the nonrelativistic  $2^3\Sigma^+$  state. More accurately the strong non-adiabatic interaction with the neighboring 2(1) and 4(1) potentials has to be taken into account. Alternately, we can view this coupling as being due to the spin-orbit interaction between the nonrelativistic  $2^3\Sigma^+$ ,  $1^3\Pi$ , and  $1^1\Pi$  potentials. In addition, we performed multi-channel calculations of the ro-vibrational structure and the vibrationally-averaged transition dipole moments to the ground state levels. The three intermediate excited states that are of interest have  $\Omega=1$  symmetry and are shown in Fig. 1 together with the ground state potentials of KRb. Panel a of Fig. 1 shows the pathway to form  $v=0$   $a^3\Sigma^+$  molecules starting from a gas of Feshbach molecules. Similarly, panel b shows the pathway to  $v=0$   $X^1\Sigma^+$  molecules.

In our multi-channel calculation we use the  $X^1\Sigma^+$  non-relativistic ground-state BO potential from Ref. [4] and the  $2^3\Sigma^+$ ,  $1^1\Pi$ , and  $1^3\Pi$  excited potentials from Ref. [8]. All three excited

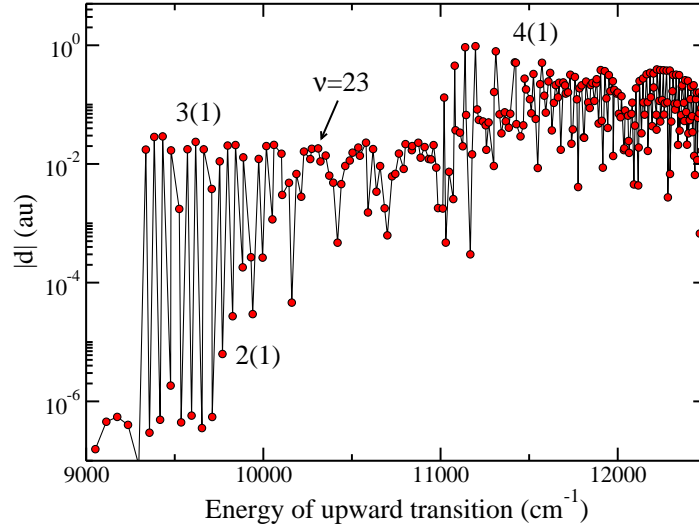


Figure 3: Transition dipole moment from the  $v=0$ ,  $J=0$   $X^1\Sigma^+$  level to the excited  $\Omega=1$  levels of the  $^{40}\text{K}^{87}\text{Rb}$  molecule as a function of the excited-state energy. Zero energy corresponds to the dissociation energy of both  $^{40}\text{K}$  and  $^{87}\text{Rb}$  in the energetically lowest hyperfine state. The bound  $v=23$  level of the  $3(1)$  potential, used as intermediate state in [2], is marked. The calculated dipole moment to the  $v=23$  level is 0.018 a.u.

potentials dissociate to the  $K(^2S)+Rb(^2P)$  limit. The previously unknown spin-orbit coupling matrix elements and electronic dipole moments are obtained from our MOL-RAS-CI calculations. For the spin-orbit interaction between  $\Omega=1$  potentials diagonal matrix elements are zero. As we will be interested in vibrational levels near the bottom of the 3(1) potential spin-orbit coupling to  $2^1\Pi$  potential can be neglected. At large  $R$  the matrix elements approach  $\Delta/3$ , where  $\Delta$  is the spin-orbit splitting of the  $^2P$  state of  $^{87}Rb$ . The dipole moments between the singlet  $X^1\Sigma^+$  and the triplet  $2^3\Sigma^+$  and  $1^3\Pi$  states are strictly zero.

Figure 3 shows the transition dipole moments between vibrational levels of the multi-channel  $\Omega = 1$  calculation described above and the  $v = 0$   $J = \ell = 0$  ro-vibrational level of the  $X^1\Sigma^+$  potential assuming our theoretical electronic dipole moment. This vibrationally-averaged dipole moment describes the downward part of the Raman transition. The vibrational averaged dipole moment from the singlet  $X^1\Sigma^+$  state is only nonzero if the multi-channel vibrational levels contains  $^1\Pi$  character. A larger character leads to a larger transition dipole moment. The start of the vibrational series of the 3(1) and 4(1) potential are clearly visible in the figure. The intermediate vibrational level used in Ref. [2] is again indicated by  $v = 23$ . From our calculation we find a dipole moment of 0.018 a.u. for the transition from this level.

## 2.2 Molecular Polarizability

The relevant property for controlling a molecule with a light field is the complex molecular dynamic polarizability  $\alpha(h\nu, \vec{\epsilon})$  as a function of radiation frequency  $\nu$  and polarization  $\vec{\epsilon}$  ( $h$  is Planck's constant).

Our results for the molecular polarizability of KRb and RbCs at very-long wavelengths corresponding to microwave frequencies are shown in Fig. 4. Unlike the  $J = 0$  rotational level, the polarizability of  $J \geq 1$  rotational levels depends on the polarization of light and the projection of  $\vec{J}$ . For microwave frequencies electric dipole transitions within the ground  $X^1\Sigma^+$  potential dominate. This  $X^1\Sigma^+$  contribution does not exist for homonuclear molecules. The resonances in the graph are due to the rotational transitions from  $J = 0$  to  $J = 1$  and from  $J = 1$  to  $J = 0$  and  $J = 2$  within the same  $v = 0$  vibrational state. The  $J = 1$  to  $J = 2$  transition occurs at a larger photon frequency. For the near-resonance frequencies the polarizabilities in Fig. 4 are approaching 1 MHz/(W/cm<sup>2</sup>), which is much larger than atomic polarizabilities of K, Rb, and Cs in the same frequency region. For example, the dynamic polarizability of a Rb atom [9] is 4 to 5 orders of magnitude smaller than the dynamic polarizability of the RbCs molecule at the same frequency.

Figure 5 shows both real and imaginary part of the polarizability of the  $v = 0, J = 0$  state of the  $X^1\Sigma^+$  potential of KRb (upper panel) and RbCs (lower panel) in the optical domain. The imaginary part is proportional to the line width of the excited states and is smaller than the real part of the polarizability for both molecules. In fact, the ratio between the real and imaginary parts of the polarizability is about  $10^7$  away from the resonances and significantly smaller ( $\sim 10^3$ ) near them. Optical potentials seen by KRb or RbCs molecules in these regions can be very deep ( $V_0/h \approx 1$  MHz) for laser intensities on the order of  $10^4$  W/cm<sup>2</sup>. At such intensities tunneling of molecules from one lattice site to another is negligible. Moreover, the decoherence time is significantly larger than 1 s.

Using our results we propose two frequency intervals in which resonant excitation is unlikely and are most easy to work with experimentally. For the lattices in an optical domain, we suggest lasers with wavelengths between  $680 \pm 35$  nm for a KRb and  $790 \pm 40$  nm for a RbCs experiment. In addition, telecommunication wavelengths between  $1.03 \pm 0.05$   $\mu\text{m}$  seem practical for both molecules.

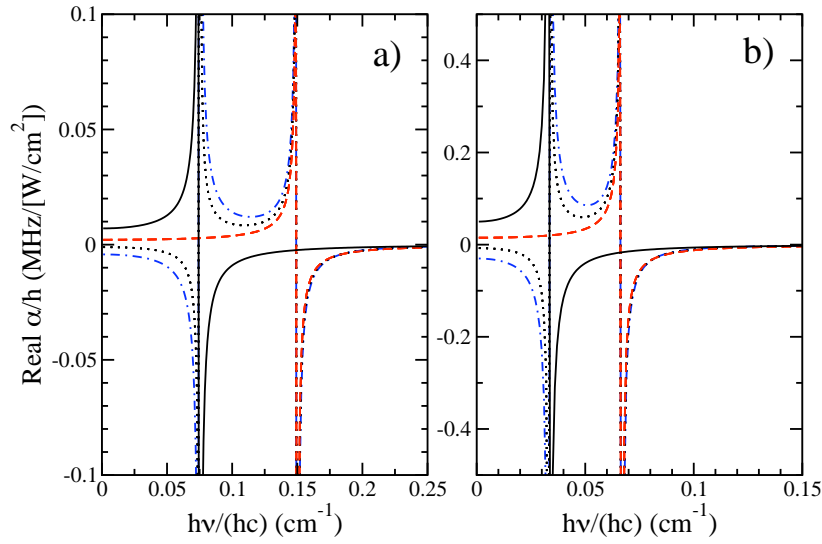


Figure 4: Dynamic polarizability for various photon polarizations of KRb (panel a) and RbCs (panel b) in the  $J = 0$  or  $J = 1$ ,  $v = 0$  rovibrational level of their  $X^1\Sigma_0^+$  electronic ground state as a function of the microwave frequency. The solid line in both panels corresponds to the polarizability of the  $J = 0$  level, which is independent of the photon polarization. All other curves are for the  $J = 1$  level. The dotted line corresponds to the polarizability of  $M=\pm 1$  magnetic sublevels illuminated by linear polarized  $\sigma_x$  or  $\sigma_y$  radiation. The dashed line relates to either  $M=\pm 1$  sublevels illuminated by  $\sigma_z$  light or the  $M = 0$  level with  $\sigma_x$  or  $\sigma_y$  light. Finally, the dashed-dotted line is obtained for  $M = 0$  levels with  $\sigma_z$  light. Note that the scale on both axes differs for the two panels.

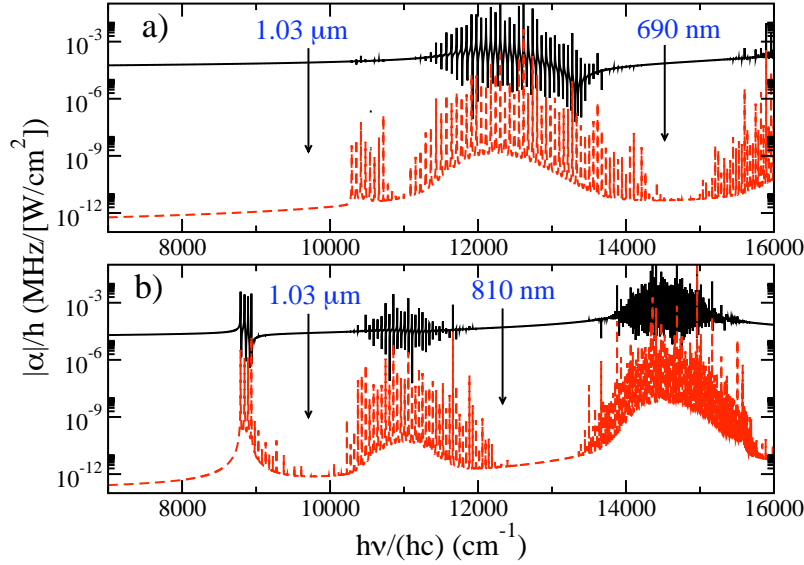


Figure 5: Real (solid line) and imaginary part (dashed line) of the dynamic polarizability of the  $v = 0, J = 0$  level of the  $X^1\Sigma^+$  state of KRb (panel a) and RbCs (panel b) as a function laser frequency. Practical laser frequencies are indicated.

We conclude by saying that despite the fact that molecules have an internal structure that is more complex than atoms, this complexity can be used to good advantage or neutralized. Microwave fields nearly resonant with rotational transitions within the molecule can lead to tunable interactions between neighboring molecules. For optical lattice potentials created by standing light waves, a careful selection of laser frequency, in regions where the Franck-Condon factors to excited vibrational levels are small, creates conditions for which the ratio of coherent to decoherent effects is large and nearly independent on the internal molecular structure. Moreover, heavy polar alkali metal molecules can be strongly confined in an optical lattice with relatively modest intensities.

### 2.3 Development of a new type of cold molecules

We have studied the electronic properties and dynamics of a new class of ultracold polar molecules created from collisions of ultracold alkali-metal Li and either an alkaline-earth or rare-earth atoms. Interest in the LiSr and LiYb molecules stems from prospects to achieve optical Feshbach tuning of scattering properties between their individual atoms without substantial loss of atoms from a trap. This photoassociative tuning becomes possible due to the existence of long-lived excited molecular states near the narrow intercombination lines of the alkaline-earth or rare-earth atoms.

Similarly, a two-photon optical Feshbach resonance can be used to couple two colliding atoms to a vibrational level of the molecular ground state. The suppressed effect of excited-state spontaneous decay might make efficient coherent molecular formation possible. Knowledge of the electronic and rovibrational properties of LiSr and LiYb will help to find optimal pathways to create ultracold



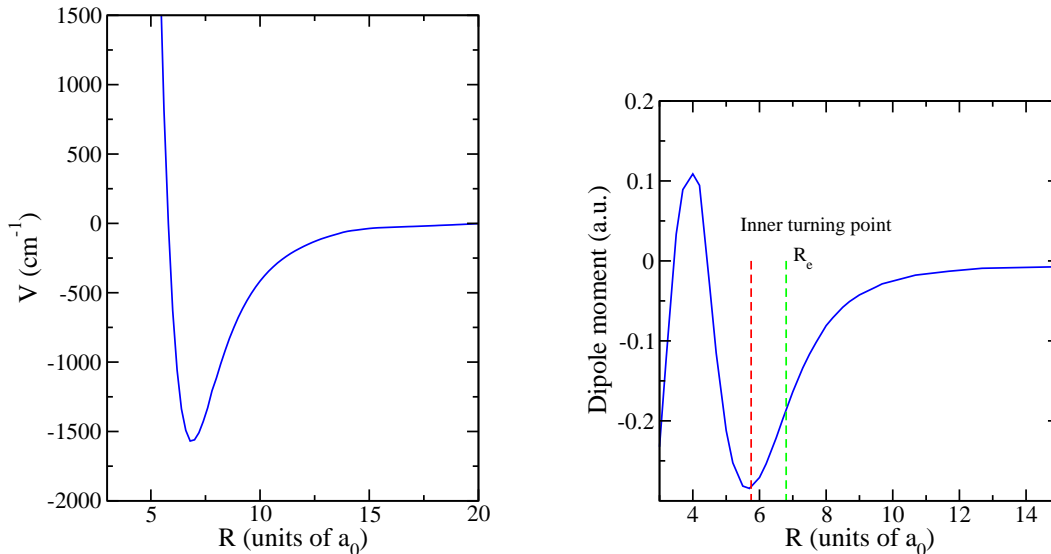


Figure 6: The potential and permanent dipole moment of the ground  $X^2\Sigma^+$  state of LiSr as a function of internuclear separation. The green and red dotted line in the right panel correspond to  $R_e$ , the position of the minimum of the potential, and the inner turning point, where the potential energy equals that at long range.

molecules by using optical Feshbach resonances or two-photon photoassociation. Such characteristics as permanent dipole moments of the ground state of these molecules, which are predicted for the first time, will determine anisotropic interactions between these molecules in an optical trap.

We have applied two different computational quantum-chemistry methods to obtain major electronic properties for molecules of our interest. The first method is the multi-reference restricted-active-space configuration interaction (MR-RAS-CI) method that includes all electrons and uses non-relativistic numerical Hartree-Fock and Sturm molecular orbitals as a basis set. The second method is the multi-reference complete-active-space configuration interaction (MR-CAS-CI) method that uses an effective core pseudopotential and Gaussian basis sets for valence electrons. We expect that a comparison of the results obtained by these two methods will help us to estimate the uncertainty of our prediction.

Both computational methods are based on non-relativistic approximation, which allows us to use large basis sets and extensive correlation interaction expansions. However, the non-relativistic description of the  $^2\Sigma_{1/2}^+$  ground state of the lighter LiMg and LiSr molecules can be more justified than for the heavier LiYb. We expect that inclusion of relativistic effects in the calculation of LiYb might change the predicted molecular parameters. We present the first results for LiSr in Fig. 6.

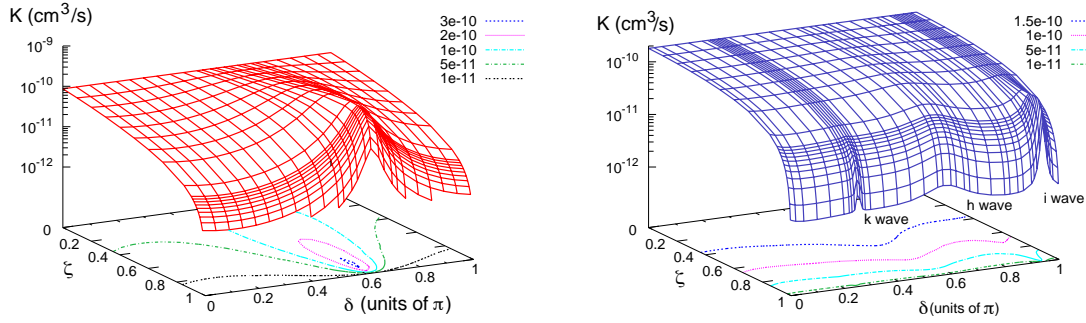


Figure 7: The inelastic loss rate for KRb (left panel) and RbCs(right panel) as a function of the short-range parameters  $\zeta$  and  $\delta$ . In both cases the molecules are in their absolute ground rovibrational state. The rates for KRb are evaluated at a collision energy of  $E/k_B = 300$  nK and that for RbCs at  $250 \mu\text{K}$ .

## 2.4 Interaction between molecules

When molecules are held in an optical dipole trap, they can come close together and collide. In fact, the molecules can react. For example it is energetically favorable for two KRb molecules in their absolute ground vibrational state to form  $\text{K}_2$  and  $\text{Rb}_2$ .

The interaction between molecules without an external electric field is dominated by the van der Waals forces. In order words, for each ro-vibrational level  $|vJM\rangle$  the interaction potential between them has the form

$$V_{\text{tot}}(R, \theta) = -\frac{C_6^{\text{iso}}}{R^6} - \frac{C_6^{\text{aniso}}}{R^6} P_2(\cos \theta) + \frac{\hbar^2 \ell(\ell + 1)}{2\mu R^2} \quad (1)$$

where  $R$  is the distance between to molecules and  $\theta$  describes the orientation of the axis that connects the molecules, where  $P_2(\cos \theta)$  is the second-order Legendre polynomial. The first two terms in this equation are the isotropic and anisotropic van der Waals interaction potentials, which are described by the isotropic  $C_6^{\text{iso}}$  and anisotropic  $C_6^{\text{aniso}}$  van der Waals coefficients. For the rotationless  $J = 0$  molecules  $C_6^{\text{aniso}}$  is zero. The last term is the centrifugal potential, where  $\ell$  is the relative orbital angular momentum of the two molecules. The interaction potential is a good approximation as long as it is smaller than the rotational energy spacing between  $|vJM\rangle$  states. At smaller  $R$  different rotational levels are coupled and, moreover, a reaction can occur. We call this separation  $R_c$ . For KRb this separation is about  $50 a_0$ .

Nevertheless, we can use this potential to set up a simple yet powerful model of the reaction rates for rotationless  $J = 0$   $v = 0$  molecules. In this case the potential is isotropic. Our model is based on the assumption that molecules, which penetrate to  $R_c$ , will be partially reflected with an amplitude  $\zeta$  and phase  $\delta$ . For  $\zeta = 0$  nothing returns from short-range while for  $\zeta = 1$  all amplitude returns. For  $R > R_c$  the molecule scatter from the attractive  $-C_6^{\text{iso}}/R^6$  potential. A priori we do not know the values for  $\zeta$  and  $\delta$ .

The value of  $C_6^{\text{iso}}$  was evaluated by integrating the dynamic polarizability over imaginary frequency. We previously evaluated the dynamic polarizability over real laser frequency in order to establish optical or magic trapping frequencies of molecules. This effort could be straight forwardly

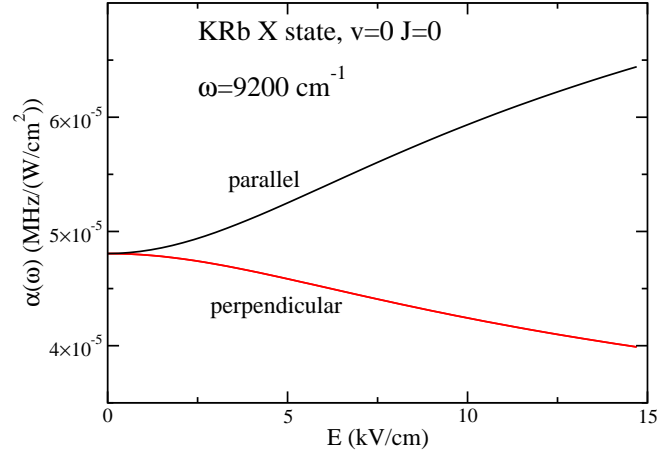


Figure 8: Anisotropic molecular polarizability of KRb in the absolute ground state as a function of external electric field. The wavelength of the trapping laser is 1090 nm.

extended to imaginary frequencies.

Figure 7 shows a three-dimensional representation of the collisional loss rate between  $v = 0$ ,  $J = 0$  KRb and RbCs molecules as a function of the short-range parameters  $\zeta$  and  $\delta$ . The collision energy for the two molecules reflects typical temperatures in experiments with these molecules. Using typical densities in ultracold experiments of around  $10^{12}$   $1/\text{cm}^3$  we find lifetimes less than a second.

Both panels in the figure show maxima as function of the short-range parameters. These maxima and thus enhancement of the loss rate is due to an interference between in- and out-going waves. For the KRb figure the loss rate has a clear maximum around  $\zeta=0.98$  and  $\delta = 0.62$ . The red dotted contour line indicates the values of short range parameters that will give a loss rate of  $2 \times 10^{-10}$   $\text{cm}^3/\text{s}$ .

The quantum interference depends on the collisional energy. For example, at a temperature of 250  $\mu\text{K}$  the resonant enhancement of the RbCs scattering rate is less pronounced. In fact, for higher temperatures the scattering rate has significant contributions from multiple partial waves  $\ell$ . In this case there are eight contributing partial waves.

For a single component Fermi gas, such as the fermionic  $^{40}\text{K}^{87}\text{Rb}$  all prepared in the same spin state,  $s$ -wave collisions can not occur and the losses are predominantly due to  $p$  wave collisions. The loss rates will be much smaller than those shown in Fig. 7, but nevertheless have a characteristic maximum.

Finally, we investigated the anisotropy of the molecular polarizability. This anisotropy occurs when both a DC electric field and trapping laser light are present. Then the polarizability of the molecules will depend on the relative orientation of the electric field and polarization of the laser light. As a result, the trapping potential will depend on this orientation. It might be possible to measure molecular trapping frequencies as a function of an external electric field.

Figure 8 shows our theoretical prediction of such dependence. The molecular dynamic polariz-

---

## Final Progress Report

---

ability is given at a trapping wavelength of 1090 nm. The curves correspond to laser polarization parallel or perpendicular to the electric field. The anisotropy appears due to mixing of the  $J = 0$  level with the  $J = 1$  levels.

## References

- [1] S. Ospelkaus, A. Peer, K.-K. Ni, J. J. Zirbel, B. Neyenhuis, S. Kotochigova, P. S. Julienne, J. Ye, and D. S. Jin, *Nature Physics* **4**, 622 (2008).
- [2] K.-K. Ni, S. Ospelkaus, M. H. G. de Miranda, A. Peer, B. Neyenhuis, J. J. Zirbel, S. Kotochigova, P. S. Julienne, D. S. Jin, and J. Ye, *Science* **322**, 231 (2008).
- [3] K. R. Berry and M. A. Duncan, *Chem. Phys. Lett.* **279**, 44 (1997).
- [4] A. Pashov, O. Docenko, M. Tamanis, R. Ferber, H. Knöckel, and E. Tiemann, *Phys. Rev. A* **76**, 022511 (2007).
- [5] W. C. Stwalley, *Eur. Phys. J. D* **31**, 221225 (2004).
- [6] J. Sage, S. Sainis, T. Bergeman, and D. DeMille, *Phys. Rev. Lett.* **94**, 203001 (2005).
- [7] T. Bergeman, A. J. Kerman, J. Sage, S. Sainis, and D. DeMille, *Eur. Phys. J. D* **31**, 179 (2004).
- [8] S. Rousseau, A. R. Allouche, and M. Aubert-Frèçon, *J. Mol. Spect.* **203**, 235 (2000).
- [9] M. S. Safronova, C. J. Williams, and C. W. Clark, *Phys. Rev. A*, **67**, 040303(R) (2003).